



Research Article

ISSN : 0975-7384
CODEN(USA) : JCPRC5

Theoretical study of lysophosphatidic acid acyltransferase 2 inhibitors

Shyamal Sharma¹, Bhaskar Bagchi¹, Subhasis Mukhopadhyay² and Asim Kumar Bothra^{3*}

¹*Cheminformatics Bioinformatics Lab, Department of Chemistry, Raiganj College (University College), P.O.- Raiganj, Dist.- Uttar Dinajpur, INDIA*

²*Bioinformatics Centre, Department of Biophysics, Molecular Biology and Bioinformatics University of Calcutta, 92 APC Road, Kolkata, INDIA*

³*Department of Chemistry, Raiganj College (University College), P.O.- Raiganj, Dist.- Uttar Dinajpur, INDIA*

ABSTRACT

AGPAT2, 1-acylglycerol-3-phosphate-o-acyltransferase2 (also known as lysophosphatidic acid acyltransferase, is a novel target for cancer therapy. There are several lysophosphatidic acid acyltransferase inhibitors. In this work different QSAR models are developed using quantum chemical parameters like HOMO, LUMO, dipole moment etc and also with topological indices like Wiener index, Harary index etc. The models are examined and it is found the model containing both electronic parameters and topological indices are suitable for screening these inhibitors which may also give an idea for initiating new inhibitors

Keywords: QSAR, lysophosphatidic acid acyltransferase 2 inhibitors, AGPAT2 enzymes, regression analysis.

INTRODUCTION

1-acylglycerol-3-phosphate-o-acyltransferase2 (also known as lysophosphatidic acid acyltransferase 2) (AGPAT2) occurs in plants, bacteria, yeast and animal cells [1]. The AGPAT2 gene issues instructions for making an enzyme that plays an important role in the growth and development of adipocytes, which are the body's fat storing cells. The AGPAT2 enzyme produces two important types of lipids glycerophospholipids and triacylglycerols. Glycerophospholipids involved in chemical signaling within cells and found in various cell membranes and triacylglycerols used in storing energy. The AGPAT2 enzyme helps to convert lysophosphatidic acid (LPA) to phosphatidic acid (PA). In another reaction PA gets converted into triacylglycerol and phosphoglycerides [2,3].

Several AGPAT2 mutations are observed in congenital generalized lipodystrophy (CGL) patients. These mutations change the structure and function of the AGPAT2 enzyme. It was suggested that the abnormal AGPAT2 enzyme may reduce the levels of triacylglycerol and phosphoglycerides in adipocytes. Thus the structure of the cell membrane would change and disrupt normal signaling within these cells [4].

In mammalian cells, AGPAT2 is found mainly in liver and heart and to a lesser extent in prostate, ovaries and testis. AGPAT2 is also found at high levels in a wide variety of tumor cells and their surrounding stroma. PA is a key lipid cofactor in cell signaling events including Raf translocation to membranes, mTOR activation, epidermal growth factor receptor (EGFR) internalization and activation of PKC ζ . However, ectopic overexpression of AGPAT2 has been shown to cooperate in activation of the Ras/Raf/Erk pathway in Xenopus oocytes and AGPAT2 seems to play a role in tumor cell survival. RNAi knock down of AGPAT2 blocked tumor cell proliferation. Hence, AGPAT2 is a novel target for cancer therapy [5,6]. There are several lysophosphatidic acid acyltransferase inhibitors, e.g., 2-

arylbenzoxazole, 2-arylbenzothiazole and 2-arylbenzimidazole analogues, new classes of isoform has been synthesized [3] and tested for antiproliferative effects in tumor cell lines in vitro. Also a group of 2,4-diamino-N4,6-diaryltriazines have been synthesized as isoform of specific inhibitors of LPAAT- β .

In this study, we intends to find correlation between biological activity and different molecular descriptors. Different QSAR (Quantitative Structure Activity Relationship) models are developed and examined which would guide the synthesis of new inhibitors.

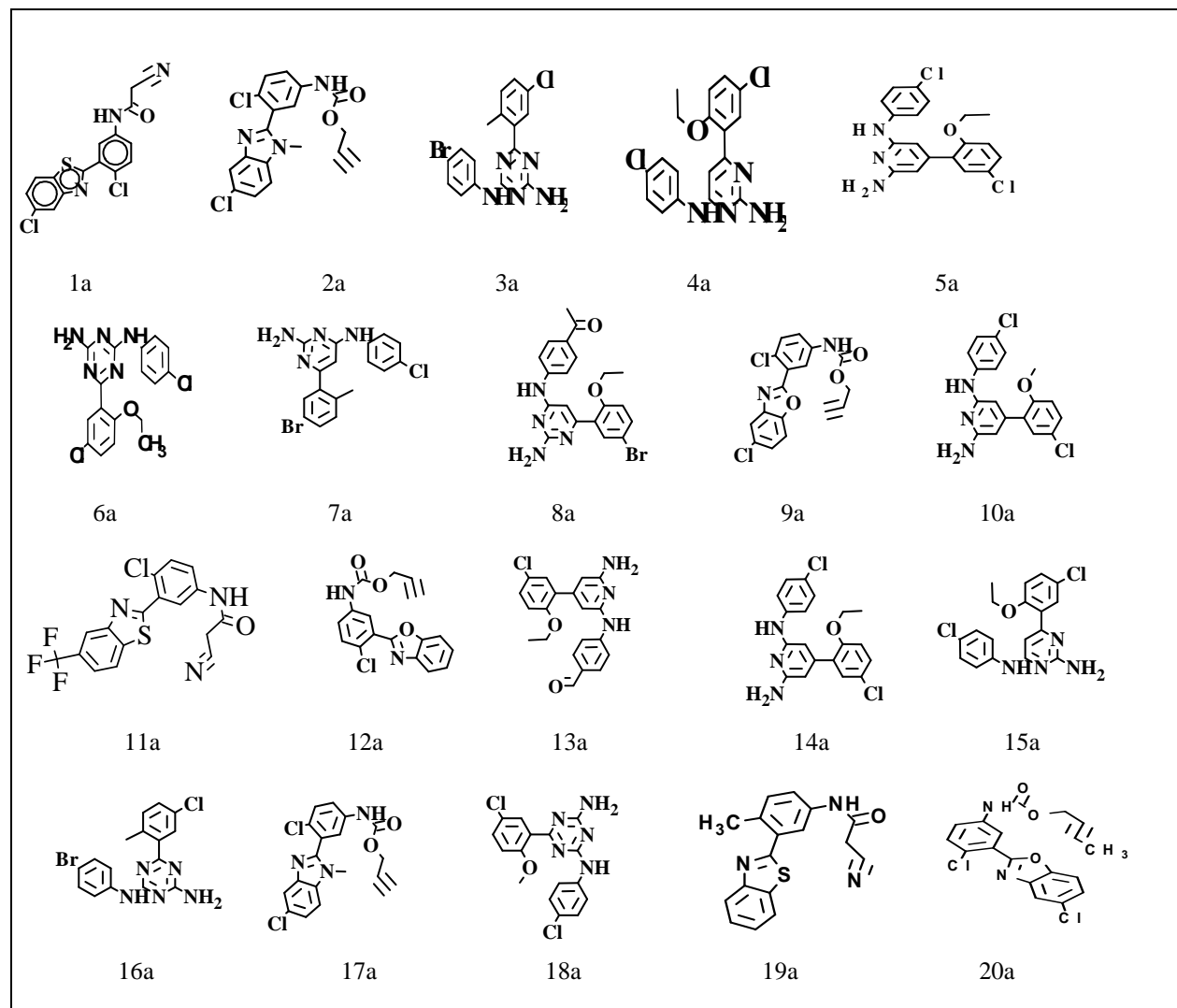
EXPERIMENTAL SECTION

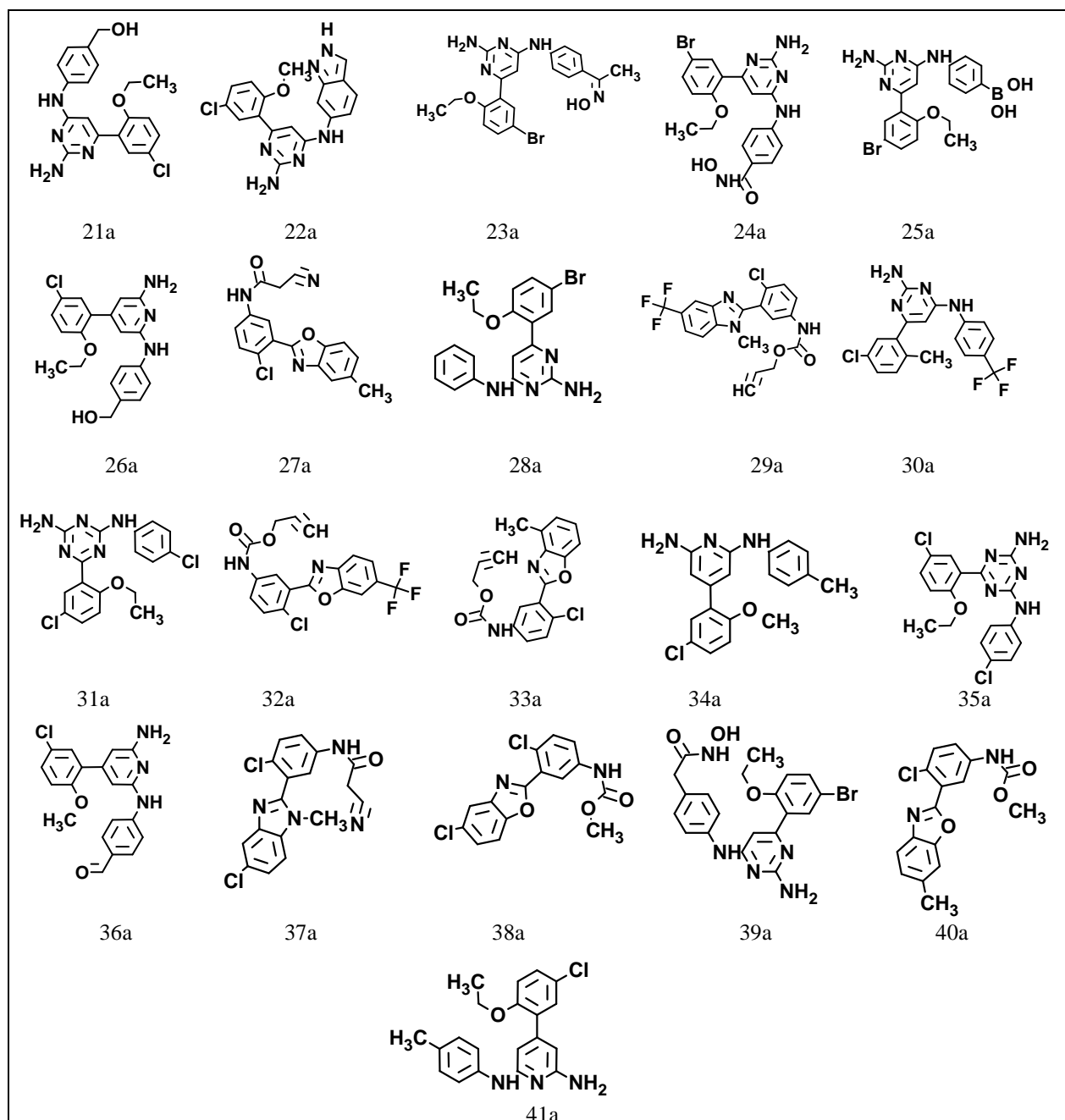
The topological indices used in this study are Wiener index (W) [7], Randiac connectivity index of first order (K_{i0}) and second order (K_{i1}) [8,9], Harary index (H) [10], Information theoretic index (I^w_D) [11,12] and Balban index (J) [13]. Calculations of quantum mechanical descriptors like HOMO energy, LUMO energy, and Dipole Moment, were performed by DFT/B3LYP calculation using the software Gamess and the basis set 6-31G (d) was used [14]. The other two liophilic parameters LogP and Molar Volume (MV) are calculated by using ACDLABS 10.0 [15].

RESULTS AND DISCUSSION

To construct the QSAR model a total of 51 compounds are taken out of which 41compounds were used as training compound and the remaining 10 compounds were taken as test compounds. Chemical structure of training and test compounds are given in Table 1 whose IC₅₀ values are taken from the site Bindingdb [16-18]. Table 2 represents the chemical structures of 10 test compounds.

Table 1 Chemical structures of 41 training set





In this study, we have divided the entire regression into two parts—one with quantum chemical indices and another with topological indices. From Table 3 it is evident that HOMO energy for the compounds ranges between -110.63 kcal/mol to -148.343 kcal/mol and LUMO energy ranges between -6.5888 kcal/mol to -38.529 kcal/mol. The correlation matrix between electronic descriptors and cytotoxic activity is presented in Table 4. It is observed that HOMO and LUMO have weak positive correlation ($r= 0.1898$ and $r= 0.2135$) with activity whereas LogP shows negative correlation ($r=-0.1853$) and dipole moment does not show any significant correlation ($r=-0.0514$).

Table 2 Chemical structures of 10 test set

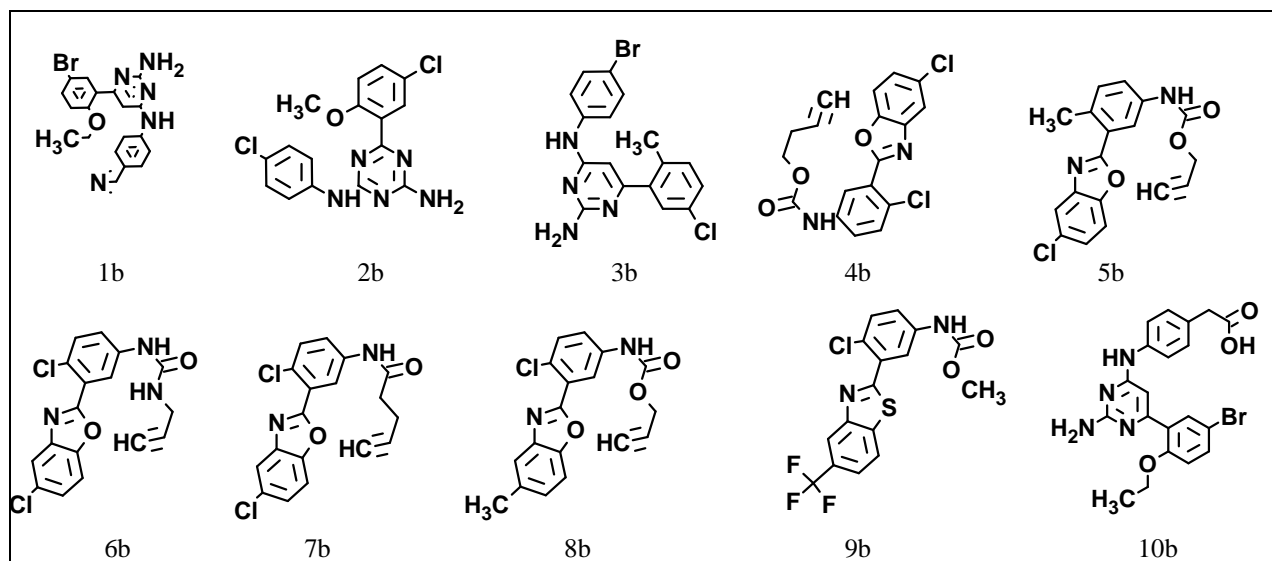


Table 3 (Quantum chemical parameters of 51 compounds under study with their IC50 value)

	HOMO (kcal/mol)	LUMO (kcal/mol)	ΔE (kcal/mol)	DM (Debye)	MV (cm ³)	LogP	IC50 (nM)
1a	-142.696	-26.8574	-115.838	7.0952	238.4	4.53	15
2a	-136.797	-31.3127	-105.484	2.682	255.9	5.34	15
3a	-128.451	-34.1365	-94.3146	2.1851	245.3	5.76	17
4a	-148.092	-25.7278	-122.364	4.9387	231.7	3.74	22
5a	-126.506	-29.1164	-97.3894	2.1017	261.6	5.16	24
6a	-122.741	-17.884	-104.857	2.4367	292.2	4.29	27
7a	-130.02	-21.2098	-108.81	3.1885	253.8	5.85	28
8a	-129.079	-26.6691	-102.41	3.9465	297.7	4.49	31
9a	-140.123	-29.7439	-110.379	5.9935	244.9	4.64	34
10a	-118.097	-11.9854	-106.112	4.0377	264.1	5.25	34
11a	-148.343	-28.8654	-119.478	4.6877	259.9	4.81	40
12a	-135.856	-27.2966	-108.559	6.1943	233	4.03	45
13a	-121.486	-22.2138	-99.272	6.3336	280.3	4.72	50
14a	-118.85	-9.7263	-109.124	2.9532	280.6	5.61	50
15a	-130.459	-22.2138	-108.245	3.4521	273.8	5.37	50
16a	-130.961	-38.529	-92.4321	6.1715	247.1	5.76	54
17a	-130.961	-38.529	-92.4321	6.1715	277.6	4.8	54
18a	-130.334	-21.9628	-108.371	2.7983	250.6	4.86	60
19a	-142.131	-22.9668	-119.164	4.1766	230.7	3.84	60
20a	-143.762	-23.2806	-120.482	4.879	261	5.47	70
21a	-124.31	-24.5356	-99.774	4.2365	275.7	4.0	75
22a	-109.814	-18.637	-91.1771	3.001	251.1	4.09	75
23a	-123.18	-35.0777	-88.1023	6.6419	299	4.5	75
24a	-131.212	-26.2926	-104.92	2.6744	287.5	3.78	80
25a	-123.368	-37.0858	-86.2825	5.3605	273.4	4.32	84
26a	-110.442	-22.2765	-88.165	4.6204	282.5	4.24	88
27a	-134.977	-32.0029	-102.974	6.9248	236	3.65	91
28a	-123.18	-19.0135	-104.167	1.8024	266.1	4.93	100
29a	-136.483	-26.8574	-109.626	4.1527	298.4	5.07	100
30a	-132.279	-23.9081	-108.371	1.4545	271.2	5.96	120
31a	-131.212	-36.3955	-94.8166	3.479	267.1	5.21	120
32a	-138.429	-33.8227	-104.606	4.7472	266.5	4.91	140
33a	-135.04	-15.3112	-119.729	5.443	249.3	4.55	140
34a	-110.63	-6.5888	-104.041	2.8849	268.4	5.16	210
35a	-130.145	-25.0376	-105.108	4.5911	267.1	5.21	230
36a	-118.725	-20.9588	-97.7659	6.1868	263.8	4.36	240
37a	-134.664	-30.7479	-103.916	2.0714	252.7	3.9	260
38a	-142.758	-26.6691	-116.089	4.5361	228.1	4.41	260
39a	-122.49	-31.8774	-90.6123	5.5847	302.4	3.76	300
40a	-134.35	-13.8052	-120.545	4.138	232.5	4.32	300
41a	-111.446	-14.0562	-97.3894	3.1924	284.9	5.52	400
1b	-132.279	-30.5597	-101.719	7.3143	266.8	4.79	17
2b	-130.083	-36.3328	-93.7499	3.2445	250.6	4.86	40
3b	-129.267	-27.5476	-101.719	3.8576	253.8	5.85	28

4b	-145.143	-19.5155	-125.627	5.01	261.4	4.93	70
5b	-138.68	-18.9507	-119.729	3.4176	249.3	4.55	99
6b	-136.358	-27.3594	-108.998	7.5272	247.4	3.91	100
7b	-141.315	-29.7439	-111.571	3.3947	255.1	4.57	100
8b	-131.714	-28.6771	-103.037	2.2133	249.3	4.55	160
9b	-144.39	-30.3714	-114.018	6.1654	256.4	5.48	170
10b	-121.109	-18.3232	-102.786	3.306	293.6	4.57	190

Table 4 (correlation matrix of activity with different quantum chemical parameters)

	HOMO (kcal/mol)	LUMO (kcal/mol)	ΔE (kcal/mol)	DM (Debye)	MV (cm ³)	LogP	Ic50 (nM)
HOMO	1	0.3716	0.7104	-0.2496	0.518	0.0708	0.1898
LUMO	0.3716	1	-0.3895	-0.3037	0.0677	0.0693	0.2135
ΔH	0.7104	-0.3895	1	-0.0174	0.4626	0.0177	0.0265
DM	-0.2496	-0.3037	-0.0174	1	-0.1194	-0.2963	-0.0514
MV	0.518	0.0677	0.4626	-0.1194	1	0.0977	0.1401
LogP	0.0708	0.0693	0.0177	-0.2963	0.0977	1	-0.1853
Ic50	0.1898	0.2135	0.0265	-0.0514	0.1401	-0.1853	1

The QSAR model (Model 1) was constructed by using the above electronic descriptors (HOMO, LUMO, difference between HOMO and LUMO, i.e., ΔE, molar volume, dipole moment, and LogP). This model shows correlation value equal to 0.3650 between predicted and experimental LogIC₅₀ and Fisher F value equal to 23.5659.

Model 1

$$\text{LnIC}_{50} = 15.873506 + (-3.7447)x \ln(-\text{Homo}) + (0.6266)x\ln(-\text{Lumo}) + (2.0876)x\ln(-\Delta E) + (-4.1497)x\text{DM} + (1.7801)x\text{MV} + (-1.4286)x\text{LogP}$$

The above analysis reveals that the electronic properties are not enough to explain the activity of these compounds. We then investigated the topological properties, and the values are presented in Table 5. The correlation matrix of the topological indices with cytotoxic activity is presented in Table 6. The information-theoretic index and Harary index shows moderate positive correlation ($r=0.3148$ and $r=0.3073$) and connectivity index show weak positive correlation ($r=0.2026$).

Table 5 (Topological indices of 51 compounds under study with their IC50 value)

	LnW	lnH	I ^w _D	J	K _{i0}	K _{i1}	Ic50 (nM)
1a	7.8995	2.5932	10.0673	1.7574	24.2815	29.5116	15
2a	8.1716	5.0438	10.3682	1.7984	26.4028	32.5339	15
3a	8.0339	5.0239	10.2237	1.9357	25.8065	31.4317	17
4a	7.8995	4.9299	10.0673	1.7574	24.2815	29.5116	22
5a	8.3223	5.1873	10.5484	2.0065	29.0136	34.8007	24
6a	8.9736	5.5236	10.2679	1.9709	37.2207	43.3446	27
7a	8.2374	5.1574	10.4551	1.8643	28.3065	33.8544	28
8a	8.8643	5.4597	11.1670	2.0349	35.5909	41.5447	31
9a	8.1062	4.999	10.2927	1.8111	25.6957	31.4579	34
10a	8.3728	5.2343	10.6074	2.0105	29.8838	35.6557	34
11a	8.1475	5.0613	10.3442	1.8384	26.7815	31.9343	40
12a	8.1062	4.999	10.2926	1.8111	25.6957	31.4579	45
13a	8.7093	5.4075	10.9799	2.0006	33.9612	39.9771	50
14a	8.5714	5.3434	10.8288	2.096	32.3838	38.1557	50
15a	8.3223	5.1872	10.5484	2.0065	29.0136	34.8007	50
16a	8.1886	5.1061	10.3970	1.8505	27.4362	32.9994	54
17a	8.3442	5.1861	10.5683	1.9802	29.066	34.7356	54
18a	8.2753	5.137	10.4925	1.7919	28.1433	33.9456	60
19a	8.1013	5.0739	10.3005	1.9329	26.7815	31.9343	60
20a	8.3717	5.1085	10.5841	1.6338	28.1957	33.7508	70
21a	8.796	5.4309	11.0724	1.9128	34.7207	40.8446	75
22a	8.5346	5.3033	10.7832	1.5302	30.8754	37.767	75
23a	8.9797	5.5171	11.2741	1.9604	37.0051	43.6207	75
24a	8.8631	5.4545	11.1452	2.0286	35.3754	42.0194	80
25a	8.8023	5.4259	11.0785	1.9025	34.5051	41.274	84
26a	8.8378	5.4711	11.1209	2.0924	35.5909	41.6997	88
27a	8.1475	5.0613	10.3442	1.8384	26.7815	31.9343	91
28a	8.5255	5.2994	10.775	1.8999	31.5136	37.3006	100
29a	8.5481	5.2989	10.7954	1.8768	31.566	37.1582	100

30a	8.4631	5.2689	10.704	1.9241	30.8065	36.277	120
31a	8.4823	5.2526	10.7238	1.8856	30.6433	36.4456	120
32a	8.3363	5.1241	10.5496	1.6985	28.1957	33.8805	140
33a	8.3204	5.1288	10.5344	1.7258	28.1957	33.8805	140
34a	8.5878	5.3402	10.844	2.0604	32.3838	38.0783	210
35a	8.4823	5.2526	10.7238	1.8856	30.6433	36.4456	230
36a	8.5207	5.3036	10.7699	1.9123	31.4612	37.4771	240
37a	8.155	5.1258	10.3636	1.9359	27.6518	32.7893	260
38a	7.9186	4.9211	10.0858	1.7264	24.2815	29.3365	260
39a	9.0223	5.5442	11.3213	1.9326	37.8754	44.5074	300
40a	8.1642	5.0534	10.3603	1.8105	26.7815	31.7592	300
41a	8.7721	5.4414	11.0491	1.9619	34.8838	40.5783	400
1b	8.5978	5.3319	10.8531	2.0389	32.2207	38.3767	17
2b	8.2753	5.137	10.4925	1.7919	28.1433	33.9456	40
3b	8.2374	5.1574	10.4551	1.8643	28.3065	33.8544	28
4b	8.3435	5.1213	10.5567	1.6766	28.1957	33.9579	70
5b	8.2922	5.1367	10.5077	1.7817	28.1957	33.8805	99
6b	8.171	5.0479	10.3672	1.7927	26.566	32.333	100
7b	8.2324	5.0977	10.4379	1.7785	27.4886	33.0116	100
8b	8.3363	5.1243	10.5496	1.6985	28.1957	33.8805	160
9b	8.1642	5.0534	10.3603	1.8105	26.7815	31.7592	170
10b	8.9171	5.4903	11.2054	2.0025	36.298	42.6861	190

Table 6 (correlation matrix of activity with different topological indices)

	LnW	lnH	I ^w _D	J	Ki ₀	Ki ₁	Ic50
LnW	1	0.6179	0.9088	0.5182	0.9927	0.9941	0.241
lnH	0.6179	1	0.5804	0.3659	0.6	0.5998	0.3073
I ^w _D	0.9088	0.5804	1	0.4928	0.8979	0.9038	0.3148
J	0.5182	0.3659	0.4928	1	0.5866	0.5615	-0.0715
Ki ₀	0.9927	0.6	0.8979	0.5866	1	0.9971	0.2265
Ki ₁	0.9941	0.5998	0.9038	0.5615	0.9971	1	0.2026
Ic50	0.241	0.3073	0.3148	-0.0715	0.2265	0.2026	1

The QSAR model (Model 2) was constructed by using the topological indices, which shows a better correlation coefficient ($r=0.6939$) and F value ($F= 50.9307$).

Model 2

$\text{LnIC}_{50} = 4.474298 + (4.0913)x\text{lnW} + (-1.3369)x\text{lnH} + (-4.3730)xI^w_D + (0.0079)xJ + (1.0556)xKi_0 + (-0.3082)xKi_1$
We have also constructed the regression model (Model 3) taking both electronic and topological parameters into account. The Model 3 yields good result ($r=0.7686$, $F=81.24$) and may be treated as a good theoretical model to judge the activity of these inhibitors.

Model 3

$\text{LnIC}_{50} = 12.472494 + 5.2750x\text{ln}(-\text{Homo}) + (-1.4500)x\text{ln}(-\text{Lumo}) + (-7.7954)x\text{Ln}(-\Delta E) + (-0.0485)x\text{DM} + (-0.6128)x\text{MV} + (-0.3644)x\text{LogP} + (1.0049)x\text{lnW} + (0.4524)x\text{lnH} + (1.9679)xI^w_D + (-3.9691)xJ + (1.8724)xKi_0 + (-1.9034)xKi_1$

Experimental and predicted activities are calculated using these models are given in Table 7.

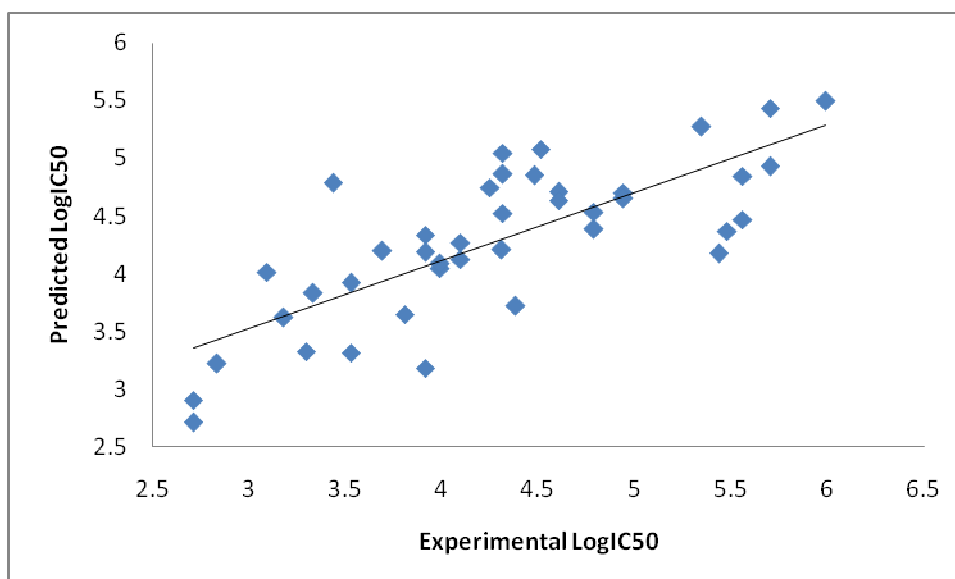
Table 7 Experimental and predicted LnIC_{50} value with different models

MODEL1 R=0.3650, F=23.5659			MODEL2 R=0.6939, F= 50.9307			MODEL3 R=0.7686, F=81.24		
Compound	Predicted	Experimental	Compound	Predicted	Experimental	Compound	Predicted	Experimental
1a	4.027696	2.7081	1a	2.704185	2.7081	1a	2.714018	2.7081
2a	3.849373	2.7081	2a	3.137285	2.7081	2a	2.904749	2.7081
3a	3.787972	2.8332	3a	3.28218	2.8332	3a	3.22181	2.8332
4a	4.194096	3.091	4a	4.168362	3.091	4a	4.012461	3.091
5a	4.050278	3.1781	5a	3.584646	3.1781	5a	3.619743	3.1781
6a	4.642795	3.2958	6a	3.322249	3.2958	6a	3.324487	3.2958
7a	3.864993	3.3322	7a	4.372326	3.3322	7a	3.832663	3.3322
8a	4.387487	3.434	8a	4.973019	3.434	8a	4.787732	3.434
9a	4.013744	3.5264	9a	3.422273	3.5264	9a	3.313235	3.5264
10a	4.577808	3.5264	10a	3.85915	3.5264	10a	3.916684	3.5264
11a	3.940705	3.6889	11a	4.553126	3.6889	11a	4.193942	3.6889
12a	4.211773	3.8067	12a	3.422063	3.8067	12a	3.647059	3.8067
13a	4.404364	3.912	13a	4.610927	3.912	13a	4.333765	3.912

14a	4.705144	3.912	14a	4.169963	3.912	14a	4.186977	3.912
15a	4.069909	3.912	15a	3.584581	3.912	15a	3.180603	3.912
16a	3.832701	3.9889	16a	4.131132	3.9889	16a	4.047159	3.9889
17a	4.251445	3.9889	17a	3.838848	3.9889	17a	4.087473	3.9889
18a	4.134275	4.0943	18a	4.175333	4.0943	18a	4.12402	4.0943
19a	4.252083	4.0943	19a	4.250648	4.0943	19a	4.269939	4.0943
20a	3.866015	4.2485	20a	5.015343	4.2485	20a	4.744141	4.2485
21a	4.531392	4.3175	21a	4.971045	4.3175	21a	5.045198	4.3175
22a	4.649634	4.3175	22a	4.405542	4.3175	22a	4.863601	4.3175
23a	4.510974	4.3175	23a	4.661225	4.3175	23a	4.524978	4.3175
24a	4.539672	4.382	24a	3.893116	4.382	24a	3.71949	4.382
25a	4.48481	4.3082	25a	4.002566	4.3082	25a	4.208763	4.3082
26a	4.672299	4.4773	26a	4.523118	4.4773	26a	4.849053	4.4773
27a	4.339666	4.5109	27a	4.553126	4.5109	27a	5.078082	4.5109
28a	4.303372	4.6052	28a	4.68827	4.6052	28a	4.707135	4.6052
29a	4.133788	4.6052	29a	5.038479	4.6052	29a	4.636949	4.6052
30a	3.815213	4.7875	30a	4.857784	4.7875	30a	4.383932	4.7875
31a	4.0354	4.7875	31a	4.445401	4.7875	31a	4.534927	4.7875
32a	4.023416	4.9416	32a	4.631887	4.9416	32a	4.702086	4.9416
33a	4.437264	4.9416	33a	4.549353	4.9416	33a	4.654349	4.9416
34a	5.232394	5.3471	34a	4.396576	5.3471	34a	5.273442	5.3471
35a	4.060759	5.4381	35a	4.445401	5.4381	35a	4.17778	5.4381
36a	4.500563	5.4806	36a	4.301346	5.4806	36a	4.369636	5.4806
37a	4.300884	5.5607	37a	4.529131	5.5607	37a	4.845577	5.5607
38a	3.999725	5.5607	38a	4.508735	5.5607	38a	4.469804	5.5607
39a	4.724357	5.7038	39a	5.015062	5.7038	39a	4.928726	5.7038
40a	4.511927	5.7038	40a	4.885173	5.7038	40a	5.43426	5.7038
41a	4.493252	5.9915	41a	5.4855	5.9915	41a	5.494472	5.9915

The correlation graph between experimental activity and predicted activity using Model 3 is given in Figure 1.

Figure 1: Correlation graph between experimental and predicted activity.



It is apparent from the results presented here that neither electronic parameters (Model 1) nor topological index (Model 2) alone can explain the cytotoxic activity of these inhibitors but a combination of these two satisfactorily predicts the activities of the compound and the combination model is a good candidate for screening these inhibitors and initiating the preparation of drugs utilising these groups of compounds.

REFERENCES

- [1] F Hong; H David; H Jack; W Singer; P Klein. *Bioorganic & Medicinal Chemistry Letters*. 2005, 15, 4703-4707.
- [2] B Gong; F Hong; C Kohm; S Jenkins; J Tulinsky; R Bhatt; P D Vries; W Jack; J W Singer; P Klein. *Bioorganic & Medicinal Chemistry Letters*. 2004, 14, 2303-2308.
- [3] B Gong; F Hong; C Kohm; L Bonham; P Klein. *Bioorganic & Medicinal Chemistry Letters*. 2004, 14, 1455-1459.

- [4] W Haquea; A Garga; A K Agarwal. *Biochemical and Biophysical Research Communications*. **2005**, 327, 446-453.
- [5] A K Agarwal; R I Barnes; A Garg. *Archives of Biochemistry and Biophysics*. **2006**, 449, 64-76.
- [6] Human Lysophosphatidic Acid Acyltransferase cDNA CLONING, EXPRESSION, AND LOCALIZATION TO CHROMOSOME, *The Journal of Biological Chemistry*. 272 (1997) 20299–20305.
- [7] H Wiener *J Am Chem Soc*. **1947**, 69, 17-20.
- [8] M Randiac *J Am Chem Soc*. **1975**, 97, 6609-6615.
- [9] L B Kier; L H Hall. Molecular connectivity in structure-activity analysis, Research studies press: Letchworth, Hertfordshire, U.K, 1986.
- [10] D Plavsic; S Nikolic; N Trinajstic; Z Mihalic. *J. Math. Chem.* **1993**, 12, 235-250.
- [11] D Bonchev; N Trinajstic. *J. Chem. Phys.* **1977**, 67, 4517-4533.
- [12] B Gong; F Hong; C Kohm; L Bonham; P Klein. *Bioorganic & Medicinal Chemistry Letters*. **2004**, 14, 1455-1459.
- [13] A T Balaban. *Chem. Phys. Lett.* **1982**, 89, 399-404.
- [14] M W Schmidt; K K Baldridge; J A Boatz; S T Elbert; M S Gordon; J H Jensen. GAMESS Version= 24 Mar 2007 (R1) from Iowa State University. *J Comput Chem*. **1993**, 14, 1347-1363.
- [15] ACD/ChemSketch Freeware, version 10.00, Advanced Chemistry Development, Inc., Toronto, ON, Canada, www.acdlabs.com, 2012.
- [16] X Chen; Y Lin; M Liu; M K Gilson. BindingDB: A Web-accessible molecular recognition database *Comb. Chem. High Throughput Screen.* **2002**, 4, 719-725.
- [17] X Chen; Y Lin; M Liu; M K Gilson. The binding database: Data management and interface design *Bioinformatics*. **2002**, 18, 130-139.
- [18] X Chen; Y Lin; M Liu; M K Gilson. The binding database: Overview and user's guide *Biopolymers/Nucleic Acid Sci.* **2002**, 61, 127-141.